Adjustable robust optimization approach for two-stage operation of energy hub-based microgrids

Adjustable Robust Optimization Approach for Two-Stage Operation of Energy Hub-Based Microgrids

Mohammad H. Shams [1], Majid Shahabi [2], Mohammad MansourLakouraj[3], Miadreza Shafie-khah [4], João P. S. Catalão [5*]

[1] *Faculty of Electrical and Computer Engineering, Babol Noshirvani University of Technology, Babol, Iran, Shams@stu.nit.ac.ir*
[2] *Faculty of Electrical and Computer Engineering, Babol Noshirvani University of Technology, Babol, Iran, Shahabi.m@nit.ac.ir*
[3] *Faculty of Electrical and Computer Engineering, Babol Noshirvani University of Technology, Babol, Iran, m.mansour349@gmail.com*
[4] *School of Technology and Innovations, University of Vaasa, 65200 Vaasa, Finland, mshafiek@uva.fi*
[5] *Faculty of Engineering of University of Porto and INESC TEC, Porto, Portugal, catalao@fe.up.pt*

***Abstract*—**Growing demand for energy carriers has led to an increased interest in developing and managing multiple energy carrier microgrids. Furthermore, the volatile nature of renewable resources as well as the uncertain electrical and thermal demands imposes significant challenges for the operation of microgrids. Motivated by this, the paper leverages a *min max min* robust framework for short-term operation of microgrids with natural gas network to capture the uncertainty of wind generation and electrical/thermal loads. The proposed model is linearized and solved using the column-and-constraint generation (C&CG) procedure that decomposes the framework into a master problem and a sub-problem. The master problem minimizes the unit commitment cost, while the sub-problem determines the dispatch cost associated with the worst realization of uncertainties via a *max min* objective function. Also, polyhedral uncertainty sets are defined with budget of uncertainty parameter that adjusts the trade-off between the operation cost and the degree of robustness. The effectiveness of the framework is assessed and discussed via a 21-node energy hub-based microgrid. It can be seen that the solution immunizes against all realizations of uncertainties, whereby increasing the budget of uncertainty and the forecast error, the system robustness is improved. Moreover, the dual variables of the sub-problem are converted to the primary variables in order to evaluate the unit commitment and energy dispatch results.

***Keywords*—**Adjustable robust approach; Energy hub; Microgrids; Operation scheduling; Uncertainty.

1. Nomenclature

Indices

t	Time, t= 1, 2, …, T
i, j	Energy carriers nodes, i= 1, 2, …, I
chp	CHPs, chp= 1, 2, …, CHP
bo	Boilers, bo= 1, 2, …, BO
hp	Heat Pumps hp=1,2,…,HP
hs	Heat storages, hs= 1, 2, …, HS
b	Batteries, b= 1, 2, …, B
wt	Wind turbines wt=1, 2, …, WT

* Corresponding author. Email: catalao@fe.up.pt

g	Natural Gas
e	Electricity
h	Heat
ch	Charge/Store energy
dis	Discharge/Withdraw energy
max	Upper limits
min	Lower limits

Variables

S	Apparent power
P	Power of energy carriers
Q	Reactive Power
ES	Stored energy in heat storages
SOC	State of charge in batteries
V	Magnitude of voltage
δ	Voltage angle
Pr	The pressure of natural gas in pipelines
SUC	Start-up cost
SDC	Shut down cost
y	Dual variables
u	On/off (charge/discharge) status (1/0)
v	Dual binary variables
f	Natural gas flow

Sets and Parameters

Γ	budget of uncertainty
$\bar{\bullet}$	forecasted value of the uncertain variable •
$\hat{\bullet}$	Error of forecasted value
$E_{\bullet}$	Forecast error of uncertain variable •
ϕ	uncertainty set
PL	Electric load
TL	Thermal load
η	Efficiency of components
K	Start-up cost constant
G_{ij}	The real part of Y_{ij}, element in microgrid admittance matrix
B_{ij}	The imaginary part of Y_{ij}, element in microgrid admittance matrix
π	Prices
COP	Coefficient of performance of heat pump

k_{ij} Coefficient of natural gas pipelines

GHV Gross Heating Value

2. Introduction

Energy hub-based microgrids are small-scale energy systems with multiple-energy carrier (MEC) infrastructure that supplies electrical and thermal loads via energy hubs [1]. The energy hub is an interface that receives energy carriers in its inputs and converts them to the consumer desired load. Utilizing the energy hubs, the flexibility as well as the complexity in the operation scheduling regime of the microgrids will be increased. On the other hand, capturing the uncertainties associated with the electrical-thermal loads and volatile nature of renewable energy resources is an essential concern of the microgrid operator (MGO) [2].

Recently, researchers have shown an increased interest in short-term operation of systems with energy hubs. In [3] a method for the energy flow problem of micro energy system is introduced to minimize the day-ahead operation costs. In this reference, the day-ahead coordinated optimal operation strategies of energy hubs are formulated as a MILP optimization problem. Reference [4] presents the short-term planning of an energy hub using a stochastic programming model considering uncertainties of wind and electricity prices. Optimal operation of MEC system is studied in the presence of demand response programs, energy market, wind generation, and storage systems considering the system uncertainties such as demands, market prices, and wind speed [5].

In [6]and [7] optimal short-term and long-term planning of energy hub systems are investigated, while the physical constraints of the energy networks are not considered. Also, authors of [8] propose a scheduling framework for multi-carrier energy microgrid; however, the DC power flow, related to the security constraint of electricity system, is considered, and other energy systems are not modelled in details. Furthermore, A two-stage stochastic method for the day-ahead operation of energy hub-based microgrid is introduced in [9] considering the electrical and natural gas network constraints. The extension of [9] is proposed in [10] capturing the risk criteria in the stochastic problem using the conditional value at risk (CVaR) approach.

The previous studies have employed stochastic methods to deal with the uncertainty in the operation scheduling of MEC systems. Despite its efficacy, stochastic methods suffer from several drawbacks. The major deficiency of these stochastic scenario-based approaches is that the hard-to-obtain historical data and consequently the probability distribution function (PDF) to generate scenarios for each uncertain variable must be available. To overcome such a drawback, the set-based robust optimization methods express the uncertainties as a crude range, rather than scenarios with explicit values [11].

In the past few years, a large amount of researches has been performed on application of robust optimization methods in unit commitment problem and optimal power flow [12-16] , operation scheduling of microgrids [17-20], and co-optimization planning of natural gas and electricity systems [21-23]. In this regard, a two-stage robust model for unit commitment problem is introduced in [24] with nodal injection uncertainty using a solution methodology based on the outer approximation technique and Benders decomposition algorithm. Reference [17] defines an adjustable robust model for microgrid planning to minimize the destructive

effects of islanding events. A mathematical problem is proposed in [20] as a robust model for operation of the CHPs, loads, and thermal storage under the uncertainty of wind speed, solar irradiation, loads, and temperature. Robust daily operation of regional-district energy system is modelled as a two-stage problem in [21]. In this reference, the first stage problem schedules the unit commitment, while the second stage solves the worst scenario. However, far too little attention has been paid to introduce a polyhedral uncertainty set-based robust model for short-term planning of energy hub-based microgrids.

The main goal of this paper is to develop an adjustable two-stage robust framework for operation scheduling of the energy hub-based microgrids while minimizing the operation costs in the worst realization of the uncertainties. In order to solve the proposed two-stage problem, column-and-constraint generation (C&CG) approach has been adopted as a solution methodology to decompose the two-stage problem. Furthermore, an extensive numerical experiment on a 21-bus microgrid has been conducted to demonstrate the merits of the proposed adjustable robust model with that of a deterministic approach.

The contributions of the paper are outlined below:

- An adjustable two-stage robust approach with polyhedral uncertainty set is introduced for the operation scheduling of the energy hub-based microgrid. Furthermore, the compromise between the robustness and the operation cost is controlled using a budget of uncertainty parameter
- A comprehensive *min max min* robust problem is suggested to minimize the operation costs, while it immunizes the solution against all realizations of the uncertainties such as electrical and thermal loads, and wind turbines generation.
- Comprehensive linearization strategies are applied to improve the performance of the adopted C&CG method, which enables the operator to solve the MILP scheduling, consisting of sub and master problems, in a very short time.
- Comprehensive physical constraints of electricity and gas networks are considered to satisfy the security limits (i.e., voltages, pressure,..) of the energy systems

The organization of the paper is as follows. The problem formulation of the proposed robust model and the solution methodology are described in sections 2 and 3, respectively. Section 4 and Section 5 present the case study and the computational results. In conclusion, Section 6 provides the paper with discussions.

2. Problem Formulation

In this paper, an adjustable robust framework for operation scheduling of energy hub-based microgrids is introduced based on the Bertsimas approach [24]. Figure 1 demonstrates the generic model of the proposed robust model. In the following, the problem formulation is represented in detail.

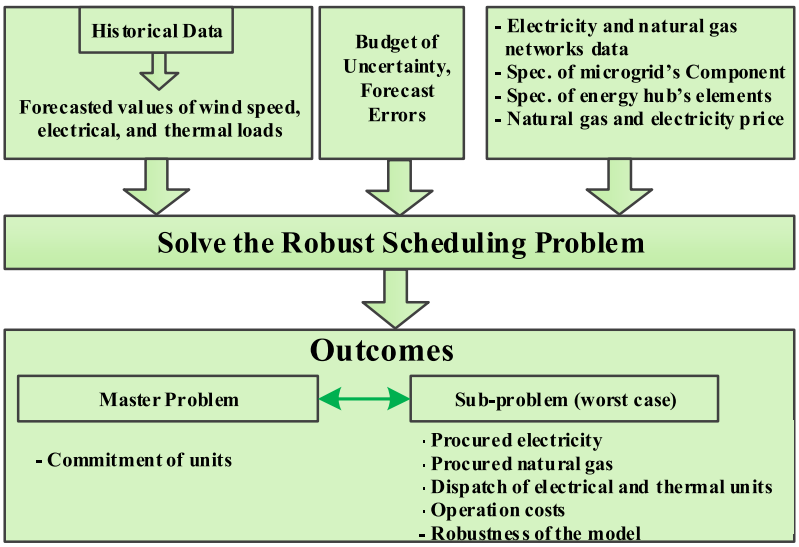

Figure 1: Generic structure of the proposed model

3.1. Uncertainty Model

In this method, given intervals are defined for each uncertain variable. In other words, during the programming, the stochastic variables can only take values within the defined uncertainty set ϕ as shown in (1). Furthermore, a parameter called "budget of uncertainty" (Γ) is considered to regulate the deviation of the stochastic variable from its nominal (forecasted) value. In better words, this parameter makes the robust model adjustable.

$$\phi := \{\bullet_i^t \epsilon \mathbb{R}^{I\times T}, : \sum_{t\epsilon T} \left|\frac{\bullet_i^t - \bar{\bullet}_i^t}{\hat{\bullet}_i^t}\right| \le \Gamma_\bullet, \qquad \bar{\bullet}_i^t - \hat{\bullet}_i^t \le \bullet_i^t \le \bar{\bullet}_i^t + \hat{\bullet}_i^t \,] \tag{1}$$

In this study, the electrical loads PL_i^t, thermal loads TL_i^t, and the wind turbine generation P_{wt}^t are considered as uncertain variables. As represented in (1), $\bar{\bullet}$ and $\hat{\bullet}$ are the forecasted value of the uncertain variable $\bullet$ and its error, respectively. In addition, it can be defined that for each uncertain variable the value of the forecast error is $E_\bullet$% of the forecasted value.

Since the extreme points of the optimization problem are on the vertices of the polyhedron of (1), we can define a set of binary variables ($\boldsymbol{v}$) to recast the continuous variables to the binary variables as (2)-(4) [25]. This transformation will be used to linearize the dual function in the solution methodology.

$$\bullet_i^t = \bar{\bullet}_i^t + \hat{\bullet}_i^t v_{i,\bullet}^{t+} - \hat{\bullet}_i^t v_{i,\bullet}^{t-} \tag{2}$$

$$v_{i,\bullet}^{t+} + v_{i,\bullet}^{t-} \le 1 \tag{3}$$

$$\sum_{t\epsilon T} (v_{i,\bullet}^{t+} + v_{i,\bullet}^{t-}) \le \Gamma_\bullet \tag{4}$$

3.2. Objective Function

The robust two-stage operation scheduling problem is defined as (5) to minimize the operation costs while the uncertain variables are in the worst case [24]. In the $min\ max\ min$ function, the max function is to find the worst case (high-cost condition) of the uncertainty set ϕ, and the first and second min functions are associated with the minimizing the unit commitment costs and the energy dispatch costs in the energy hub-based microgrid. In other words, the first part of the objective function is associated with minimizing the start-up and shut down costs of unit ω including CHP, heat pumps, and boilers. The second part minimizes the cost of purchased natural gas and electricity as well as the dispatch costs in the worst case realization of uncertain data.

$$\min_{u}\left(\sum_{t\epsilon T}\sum_{\omega\epsilon\Omega}[SUC_{\omega}^{t}+SDC_{\omega}^{t}]+\max_{\phi}\min_{P_{e}^{t},P_{g}^{t},P_{\omega}^{t}}\sum_{t\epsilon T}\{P_{e,grid}^{t}\pi_{e}^{t}+P_{g,net}^{t}\pi_{g}^{t}\}\right) \quad (5)$$

3.3. Constraints

Equations (6)-(42) demonstrate the constraints of the proposed robust scheduling model. In these constraints, the variables $y_{n}^{t,m}$ represent the dual variable n associated with the element m in the microgrid at time t. The constraints of start-up and shut down cost of unit ω are shown in (6), (7). Constraints (8), (9) limit the amount of purchased natural gas and electricity from the main grid. The limitations of procured energy from the CHPs, boilers, and heat pumps are demonstrated in (10)-(13), respectively. The equations and constraints of batteries and heat storages are shown in (14)-(21), respectively. Equations (22)-(25) present the natural gas balance in the energy hubs. The active and reactive power equations in energy hubs are shown in (26), (27) and similarly the thermal energy balance in energy hubs are presented in (28). The equations of linear power flow and constraints are described in (29)-(36) based on the model defined in [26]. Finally, the linear model of the natural gas flow equations and limitations are represented in (37)-(42) [9].

$$SUC_{\omega}^{t}\geq KU_{\omega}(u_{\omega}^{t}-u_{\omega}^{t-1})\geq 0 \quad (6)$$

$$SDC_{\omega}^{t}\geq KD_{\omega}(u_{\omega}^{t-1}-u_{\omega}^{t})\geq 0 \quad (7)$$

$$P_{grid}^{min}\leq P_{e,grid}^{t}\leq P_{grid}^{max}\ :y_{1}^{t},y_{2}^{t} \quad (8)$$

$$0\leq P_{g,net}^{t}\leq P_{g}^{max}\ :y_{3}^{t} \quad (9)$$

$$u_{chp}^{t}P_{e,chp}^{min}\leq P_{e,chp}^{t}\leq P_{e,chp}^{max}u_{chp}^{t}\ :y_{4}^{t,chp},y_{5}^{t,chp} \quad (10)$$

$$u_{chp}^{t}P_{h,chp}^{min}\leq P_{h,chp}^{t}\leq P_{h,chp}^{max}u_{chp}^{t}\ :y_{6}^{t,chp},y_{7}^{t,chp} \quad (11)$$

$$u_{bo}^{t}P_{bo}^{min}\leq P_{bo}^{t}\leq P_{bo}^{max}u_{bo}^{t}\ :y_{8}^{t,bo},y_{9}^{t,bo} \quad (12)$$

$$u_{hp}^{t}P_{hp}^{min} \le P_{hp}^{t} \le P_{hp}^{max}u_{hp}^{t} \quad : y_{10}^{t,hp}, y_{11}^{t,hp} \tag{13}$$

$$SOC_{b}^{t} - SOC_{b}^{t-1} - \eta_{b}^{ch}P_{b,ch}^{t} + 1/\eta_{b}^{dis}P_{b,dis}^{t} = 0 \quad : y_{12}^{t,b} \tag{14}$$

$$SOC_{b}^{min} \le SOC_{b}^{t} \le SOC_{b}^{max} \quad : y_{13}^{t,b}, y_{14}^{t,b} \tag{15}$$

$$0 \le P_{b,ch}^{t} \le P_{b,ch}^{max} \quad : y_{15}^{t,b} \tag{16}$$

$$0 \le P_{b,dis}^{t} \le P_{b,dis}^{max} \quad : y_{16}^{t,b} \tag{17}$$

$$ES_{hs}^{t} - ES_{hs}^{t-1} - \eta_{hs}^{st}P_{hs,st}^{t} + 1/\eta_{hs}^{wd}P_{hs,wd}^{t} = 0 \quad : y_{17}^{t,hs} \tag{18}$$

$$ES_{hs}^{min} \le ES_{hs}^{t} \le ES_{hs}^{max} \quad : y_{18}^{t,hs}, y_{19}^{t,hs} \tag{19}$$

$$0 \le P_{hs,st}^{t} \le P_{hs,st}^{max} \quad : y_{20}^{t,hs} \tag{20}$$

$$0 \le P_{hs,wd}^{t} \le P_{hs,wd}^{max} \quad : y_{21}^{t,hs} \tag{21}$$

$$P_{e,chp}^{t} - \eta_{e,chp}P_{g,chp}^{t} = 0 \quad : y_{22}^{t,chp} \tag{22}$$

$$P_{h,chp}^{t} - \eta_{h,chp}P_{g,chp}^{t} = 0 \quad : y_{23}^{t,chp} \tag{23}$$

$$P_{bo}^{t} - \eta_{bo}P_{g,bo}^{t} = 0 \quad : y_{24}^{t,bo} \tag{24}$$

$$P_{g,i}^{t} - \sum_{chp\epsilon CHP_i} P_{g,chp}^{t} - \sum_{bo\epsilon BO_i} P_{g,bo}^{t} = 0 \quad : y_{25}^{t,i} \tag{25}$$

$$\sum_{chp\epsilon CHP_i} P_{e,chp}^{t} + \sum_{b\epsilon B_i}\left(P_{b,dis}^{t} - P_{b,ch}^{t}\right) - \sum_{hp\epsilon HP_i} P_{hp}^{t} = P_{e,i}^{t} + PL_{i}^{t} - \sum_{wt\epsilon WT_i} P_{wt}^{t} \quad : y_{26}^{t,i} \tag{26}$$

$$\sum_{chp\epsilon CHP_i} Q_{e,chp}^{t} - \sum_{hp\epsilon HP_i} Q_{hp}^{t} = Q_{e,i}^{t} + QL_{i}^{t} \quad : y_{27}^{t,i} \tag{27}$$

$$\sum_{chp\epsilon CHP_i} P_{h,chp}^{t} + \sum_{bo\epsilon BO_i} P_{bo}^{t} + \sum_{hp\epsilon HP_i} COP_{hp}P_{hp}^{t} + \sum_{hs\epsilon HS_i}\left(P_{hs,wd}^{t} - P_{hs,st}^{t}\right) = TL_{i}^{t} \quad : y_{28}^{t,i} \tag{28}$$

$$P_{e,ij}^{t} = G_{ij}\left(V_{j}^{t} - V_{i}^{t}\right) + B_{ij}\left(\delta_{i}^{t} - \delta_{j}^{t}\right) \quad : y_{29}^{t,i,j} \tag{29}$$

$$Q_{e,ij}^{t} = B_{ij}\left(V_{i}^{t} - V_{j}^{t}\right) + G_{ij}\left(\delta_{i}^{t} - \delta_{j}^{t}\right) \quad : y_{30}^{t,i,j} \tag{30}$$

$$S_{e,ij}^{t} = P_{e,ij}^{t} + \xi_{ij}Q_{e,ij}^{t} \quad : y_{31}^{t,i,j} \tag{31}$$

$$\left|S_{e,ij}^{t}\right| \le S_{e,ij}^{max} \quad : y_{32}^{t,i,j}, y_{33}^{t,i,j} \tag{32}$$

$$V_i^{min} \le V_i^t \le V_i^{max} \quad : y_{34}^{t,i}, y_{35}^{t,i} \tag{33}$$

$$P_{e,i}^t = \sum_{j \epsilon J_i} P_{e,ij}^t \quad : y_{36}^{t,i} \tag{34}$$

$$Q_{e,i}^t = \sum_{j \epsilon J_i} Q_{e,ij}^t \quad : y_{37}^{t,i} \tag{35}$$

$$P_{e,grid}^t = -\sum_{i \epsilon I} P_{e,i}^t \quad : y_{38}^t \tag{36}$$

$$f_{ij}^t = k_{ij} \frac{(Pr_i^t Pr_i' - Pr_j^t Pr_j')}{\sqrt{\left|(Pr_i')^2 - (Pr_j')^2\right|}} \quad : y_{39}^{t,i,j} \tag{37}$$

$$\left|f_{ij}^t\right| \le f_{ij}^{max} \quad : y_{40}^{t,i,j}, y_{41}^{t,i,j} \tag{38}$$

$$Pr_i^{min} \le Pr_i^t \le Pr_i^{max} \quad : y_{42}^{t,i}, y_{43}^{t,i} \tag{39}$$

$$f_i^t = \sum_{j \epsilon J_i} f_{ij}^t \quad : y_{44}^{t,i} \tag{40}$$

$$P_{g,i}^t = GHV f_i^t \quad : y_{45}^{t,i} \tag{41}$$

$$P_{g,net}^t = \sum_{i \epsilon I} P_{g,i}^t \quad : y_{46}^t \tag{42}$$

3. Solution Methodology

The general form of the proposed robust objective function and constraints are shown in (43)-(45). Where $\boldsymbol{x}$ is the matrix of binary variables associated with commitment of units, $\boldsymbol{z}$ is the matrix of dispatch variables, and $\boldsymbol{\varphi}$ is the matrix of uncertain variables. Other matrices including $\boldsymbol{A}, \boldsymbol{B}, \boldsymbol{b^T}, \boldsymbol{c^T}, \boldsymbol{f}, \boldsymbol{F}, \boldsymbol{g}, \boldsymbol{G}$ are the constant coefficients of matrices.

$$\min_{\boldsymbol{x}} \left(\boldsymbol{c^T x} + \max_{\boldsymbol{\varphi}} \min_{\boldsymbol{z}} \boldsymbol{b^T z} \right) \tag{43}$$

$$\text{s.t.} \quad \boldsymbol{Fx} \le \boldsymbol{f}, \boldsymbol{x}\ binary \tag{44}$$

$$\boldsymbol{Ax} + \boldsymbol{Bz} \le \boldsymbol{g} - \boldsymbol{G\varphi} \quad \forall \boldsymbol{z} \epsilon \Lambda(\boldsymbol{x}, \boldsymbol{\varphi}) \tag{45}$$

The objective function (43) in the form of $min\ max\ min$ problem cannot be solved using the straight forward methods. In this paper, as shown in Figure 2, using the C&CG method [27] and the strong duality theory [28] the problem has been decomposed and consequently solved.

In the proposed algorithm, the problem is decomposed into a master problem and a sub-problem. In the master problem the optimal commitment of units is determined using (46)-(49) where γ is an auxiliary variable.

$$\min_{x,\gamma} \boldsymbol{c}^T\boldsymbol{x} + \gamma \tag{46}$$

$$\text{s.t.} \quad \gamma \geq \boldsymbol{b}^T\boldsymbol{z}_k \tag{47}$$

$$\boldsymbol{F}\boldsymbol{x} \leq \boldsymbol{f}, \boldsymbol{x}\ binary \tag{48}$$

$$\boldsymbol{A}\boldsymbol{x} + \boldsymbol{B}\boldsymbol{z}_k \leq \boldsymbol{g} - \boldsymbol{G}\boldsymbol{\varphi}_k^*, \qquad \forall\, \boldsymbol{z}\epsilon\Lambda(\boldsymbol{x}, \boldsymbol{\varphi}), \boldsymbol{\varphi}\epsilon\boldsymbol{\phi} \tag{49}$$

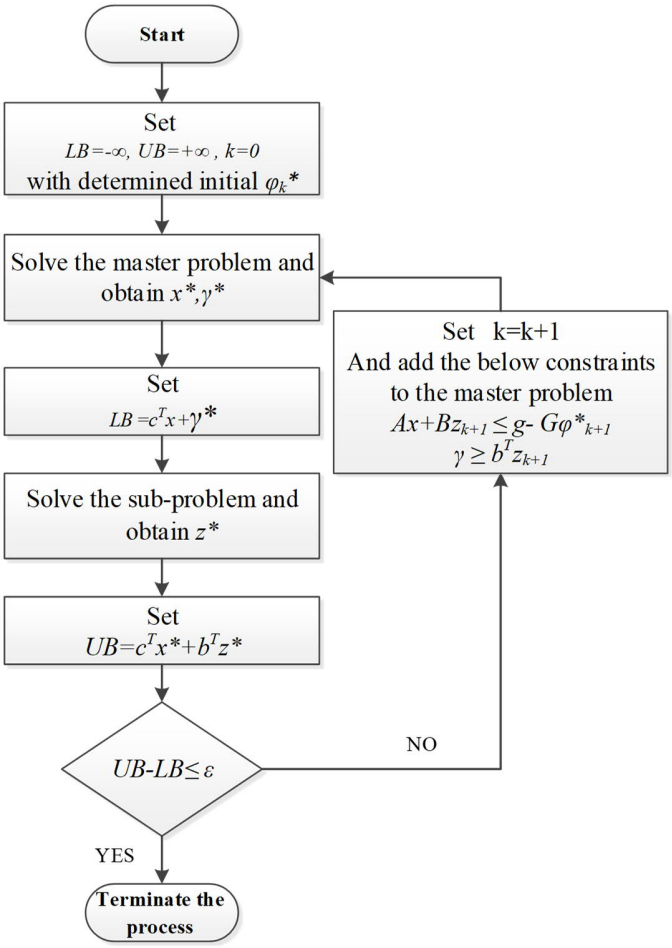

Figure 2: Solution algorithm of the proposed robust optimization problem

The optimal dispatch of energy carriers is obtained by the sub-problem using the given binary variables from the master problem as (50)-(51).

$$\max_{\boldsymbol{\varphi}} \min_{\boldsymbol{z}} \boldsymbol{b}^T\boldsymbol{z} \tag{50}$$

$$\text{s.t.} \quad \boldsymbol{A}\boldsymbol{x}^* + \boldsymbol{B}\boldsymbol{z} \leq \boldsymbol{g} - \boldsymbol{G}\boldsymbol{\varphi}_{k+1}, \forall\, \boldsymbol{z}\epsilon\Lambda(\boldsymbol{x}, \boldsymbol{\varphi}), \boldsymbol{\varphi}_{k+1}\epsilon\boldsymbol{\phi} \tag{51}$$

The $max-min$ sub-problem cannot be solved using simple methods. So, using the strong duality theory, this objective function has been reformed to a single max function as $\underset{\boldsymbol{y},\boldsymbol{\varphi}}{max}\ \boldsymbol{y^T}(\boldsymbol{g}-\boldsymbol{G\varphi}-\boldsymbol{Ax^*})$ subject to $\boldsymbol{By^T}\leq\boldsymbol{b^T}$ where $\boldsymbol{y^T}$ is the matrix of dual variables. Equation (52) represents the general model of the dual objective function.

$$
\begin{aligned}
&\max_{y,\phi}\sum_{t\epsilon T}\Big[P_{grid}^{min}\,y_1^t+P_{grid}^{max}\,y_2^t+P_g^{max}\,y_3^t \\
&+\sum_{chp\epsilon CHP}u_{chp}^{t*}\begin{Bmatrix}P_{e,chp}^{min}\,y_4^{t,chp}+P_{e,chp}^{max}\,y_5^{t,chp}\\+P_{h,chp}^{min}\,y_6^{t,chp}+P_{h,chp}^{max}\,y_7^{t,chp}\end{Bmatrix} \\
&+\sum_{bo\epsilon BO}u_{bo}^{t*}\left\{P_{bo}^{min}\,y_8^{t,bo}+P_{bo}^{max}\,y_9^{t,bo}\right\} \\
&+\sum_{hp\epsilon HP}u_{hp}^{t*}\left\{P_{hp}^{min}\,y_{10}^{t,hp}+P_{hp}^{max}\,y_{11}^{t,hp}\right\} \\
&+\sum_{b\epsilon B}\begin{Bmatrix}SOC_b^{min}\,y_{13}^{t,bo}+SOC_b^{max}\,y_{14}^{t,bo}\\+P_{b,ch}^{max}\,y_{15}^{t,b}+P_{b,dis}^{max}\,y_{16}^{t,b}\end{Bmatrix} \\
&+\sum_{hs\epsilon HS}\begin{Bmatrix}ES_{hs}^{min}\,y_{18}^{t,hs}+ES_{hs}^{max}\,y_{19}^{t,hs}\\+P_{hs,st}^{max}\,y_{20}^{t,hs}+P_{hs,wd}^{max}\,y_{21}^{t,hs}\end{Bmatrix} \\
&+\sum_{i\epsilon I}\begin{Bmatrix}\left(PL_i^t-\sum_{wt\epsilon WT_i}P_{wt}^t\right)y_{26}^{t,i}\\+QL_i^t\,y_{27}^{t,i}+TL_i^t\,y_{28}^{t,i}\end{Bmatrix} \\
&+\sum_{i,j\epsilon I}\begin{Bmatrix}-S_{e,ij}^{max}\,y_{32}^{t,i,j}+S_{e,ij}^{max}\,y_{33}^{t,i,j}\\-f_{ij}^{max}\,y_{40}^{t,i,j}+f_{ij}^{max}\,y_{41}^{t,i,j}\end{Bmatrix} \\
&+\sum_{i\epsilon I}\begin{Bmatrix}V_i^{min}\,y_{34}^{t,i}+V_i^{max}\,y_{35}^{t,i}\\+Pr_i^{min}\,y_{42}^{t,i}+Pr_i^{max}\,y_{43}^{t,i}\end{Bmatrix}\Big]
\end{aligned}
\tag{52}
$$

As shown in the seventh line of the dual objective function (52), the problem consists of bilinear terms in case of $\boldsymbol{y^T G\varphi}$ in the general form that are $PL_i^t\,y_{26}^{t,i}$, $P_{wt}^t\,y_{26}^{t,i}$, and $TL_i^t\,y_{28}^{t,i}$. By replacing the equations of (1) into the dual objective function, we have some terms as $\boldsymbol{yv}$ where $\boldsymbol{y}$ and $\boldsymbol{v}$ are continuous and binary variables, respectively. Using the big-M method, the max problem is changed into a linear problem that can be solved using an MILP approaches. In this method, M is a sufficient large number.

Equations (53)-(80) show the implementation of the dual constraints. Based on the duality theory, the number of inequality constraints in the main problem is the same as the number of variables in the dual problem and consequently the number of variables in the main problem is equal to the number of inequality constraints in the dual problem. As shown, in this paper since the operation scheduling is for the day-ahead 24 hours, there are 24×28 variables in the main problem and accordingly the same

number of constraints in the dual problem. In the following, the related main variables of dual constraints are noted for more clarifications.

$$y_1^t + y_2^t + y_{38}^t = \pi_e^t \quad : P_{e,grid}^t \tag{53}$$

$$y_3^t + y_{46}^t \le \pi_g^t \quad : P_{g,net}^t \tag{54}$$

$$y_4^{t,chp} + y_5^{t,chp} + y_{22}^{t,chp} + \sum_{i \epsilon CHP_i} y_{26}^{t,i} \le 0 \quad : P_{e,chp}^t \tag{55}$$

$$y_6^{t,chp} + y_7^{t,chp} + y_{23}^{t,chp} + \sum_{i \epsilon CHP_i} y_{28}^{t,i} \le 0 \quad : P_{h,chp}^t \tag{56}$$

$$y_8^{t,bo} + y_9^{t,bo} + y_{24}^{t,bo} + \sum_{i \epsilon BO_i} y_{28}^{t,i} \le 0 \quad : P_{bo}^t \tag{57}$$

$$y_{10}^{t,hp} + y_{11}^{t,hp} - \sum_{i \epsilon HP_i} y_{26}^{t,i} + \sum_{i \epsilon HP_i} COP_{hp}\, y_{28}^{t,i} \le 0 \quad : P_{hp}^t \tag{58}$$

$$y_{12}^{t,b} - y_{12}^{t-1,b} + y_{13}^{t,b} + y_{14}^{t,b} \le 0 \quad : SOC_b^t \tag{59}$$

$$-\eta_b^{ch}\, y_{12}^{t,b} + y_{15}^{t,b} - \sum_{i \epsilon B_i} y_{26}^{t,i} \le 0 \quad : P_{b,ch}^t \tag{60}$$

$$1/\eta_b^{dis}\, y_{12}^{t,b} + y_{16}^{t,b} + \sum_{i \epsilon B_i} y_{26}^{t,i} \le 0 \quad : P_{b,dis}^t \tag{61}$$

$$y_{17}^{t,hs} - y_{17}^{t-1,hs} + y_{18}^{t,hs} + y_{19}^{t,hs} \le 0 \quad : ES_{hs}^t \tag{62}$$

$$-\eta_{hs}^{st}\, y_{17}^{t,hs} + y_{20}^{t,hs} - \sum_{i \epsilon HS_i} y_{28}^{t,i} \le 0 \quad : P_{hs,st}^t \tag{63}$$

$$1/\eta_{hs}^{wd}.y_{17}^{t,hs} + y_{21}^{t,hs} + \sum_{i \epsilon HS_i} y_{28}^{t,i} \le 0 \quad : P_{hs,wd}^t \tag{64}$$

$$-\eta_{e,chp}\, y_{22}^{t,chp} - \eta_{h,chp}\, y_{23}^{t,chp} - \sum_{i \epsilon CHP_i} y_{25}^{t,i} \le 0 \quad : P_{g,chp}^t \tag{65}$$

$$-\eta_{bo}\, y_{24}^{t,bo} - \sum_{i \epsilon BO_i} y_{25}^{t,i} \le 0 \quad : P_{g,bo}^t \tag{66}$$

$$y_{25}^{t,i} + y_{45}^{t,i} - y_{46}^t \le 0 \quad : P_{g,i}^t \tag{67}$$

$$-y_{26}^{t,i} + y_{36}^{t,i} - y_{38}^t \le 0 \quad : P_{e,i}^t \tag{68}$$

$$-y_{27}^{t,i} + y_{37}^{t,i} \le 0 \quad : Q_{e,i}^t \tag{69}$$

$$y_{29}^{t,i,j} - y_{31}^{t,i,j} - \sum_{i \epsilon J_i} y_{36}^{t,i} \le 0 \quad : P_{e,ij}^t \tag{70}$$

$$y_{30}^{t,i,j} - \xi_{ij}\, y_{31}^{t,i,j} - \sum_{i \epsilon J_i} y_{37}^{t,i} \leq 0 \quad : Q_{e,ij}^{t} \tag{71}$$

$$y_{31}^{t,i,j} + y_{32}^{t,i,j} + y_{33}^{t,i,j} \leq 0 \quad : S_{e,ij}^{t} \tag{72}$$

$$G_{ij}\, y_{29}^{t,i,j} - B_{ij}\, y_{30}^{t,i,j} + y_{34}^{t,i} + y_{35}^{t,i} \leq 0 \quad : V_i^t \tag{73}$$

$$-G_{ij}\, y_{29}^{t,i,j} + B_{ij}\, y_{30}^{t,i,j} + y_{34}^{t,i} + y_{35}^{t,i} \leq 0 \quad : V_j^t \tag{74}$$

$$-B_{ij}\, y_{29}^{t,i,j} - G_{ij}\, y_{30}^{t,i,j} \leq 0 \quad : \delta_i^t \tag{75}$$

$$B_{ij}\, y_{29}^{t,i,j} + G_{ij}\, y_{30}^{t,i,j} \leq 0 \quad : \delta_j^t \tag{76}$$

$$y_{39}^{t,i,j} + y_{40}^{t,i,j} + y_{41}^{t,i,j} - \sum_{i \epsilon J_i} y_{44}^{t,i} \leq 0 \quad : f_{ij}^t \tag{77}$$

$$y_{44}^{t,i} - GHV\, y_{45}^{t,i} \leq 0 \quad : f_i^t \tag{78}$$

$$-k_{ij}\, \frac{Pr_i'\, y_{39}^{t,i,j}}{\sqrt{\left|(Pr_i')^2 - (Pr_j')^2\right|}} + y_{42}^{t,i} + y_{43}^{t,i} \leq 0 \quad : Pr_i^t \tag{79}$$

$$k_{ij}\, \frac{Pr_j'\, y_{39}^{t,i,j}}{\sqrt{\left|(Pr_i')^2 - (Pr_j')^2\right|}} + y_{42}^{t,i} + y_{43}^{t,i} \leq 0 \quad : Pr_j^t \tag{80}$$

4. Case Study and Description of Microgrid Test System

In order to assess the proposed robust model, a 21-node microgrid with natural gas infrastructure is considered as a test case in Figure 3. In this system, thermal and electrical loads are provided by 6 energy hubs. The specifications of the natural gas pipelines, electrical lines, and characteristics of resources in the MEC microgrid are represented in Appendix [29]. The efficiency of withdrawing and storing energy in the heat storages are 0.9. Also, the efficiency of discharging and charging the battery are 0.95. The permissible flow rate and the pressure range of natural gas is 420 $m^3/hour$ and 54-66 $Psig$, respectively. The acceptable voltage magnitude is between 0.95-1.05 $p.u.$. The base values of apparent power is 10 MVA and it is 20 kV for voltage magnitude.

Figure 4 demonstrates the model of the energy hub. The elements of this energy hub are boiler, transformer, CHP, heat storage, heat pump, and battery. Figure 5 and Figure 6 illustrate the forecasted electrical/ thermal demands, day-ahead electricity prices, and forecasted wind speed, respectively. It is assumed that the natural gas price is constant during the next day and is equal to 20 $\$/MWh$.

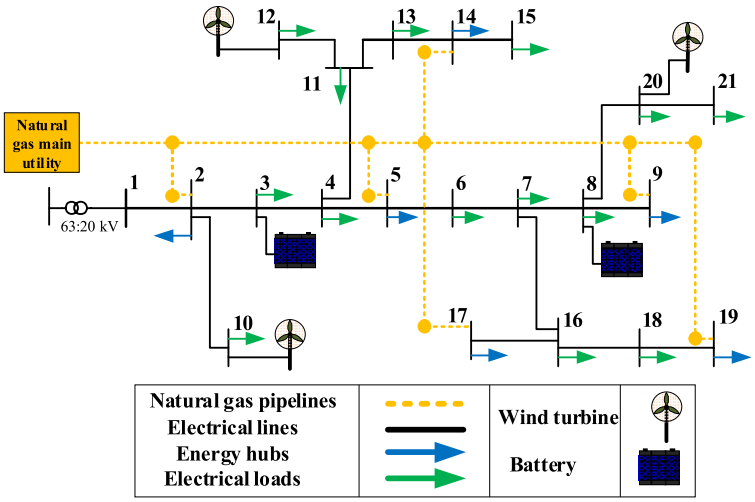

Figure 3: Microgrid under study

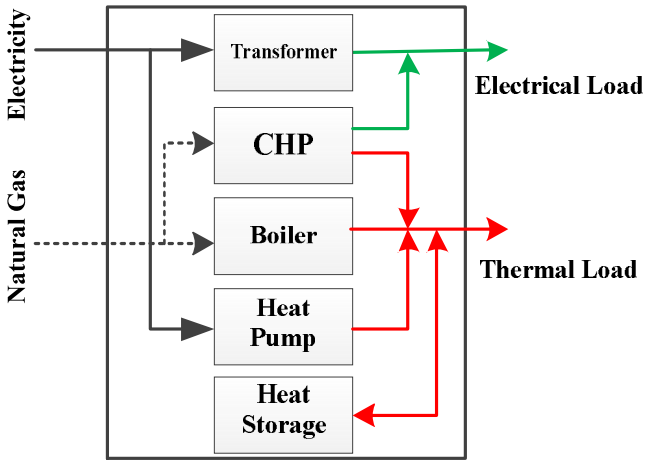

Figure 4: Proposed energy hub model

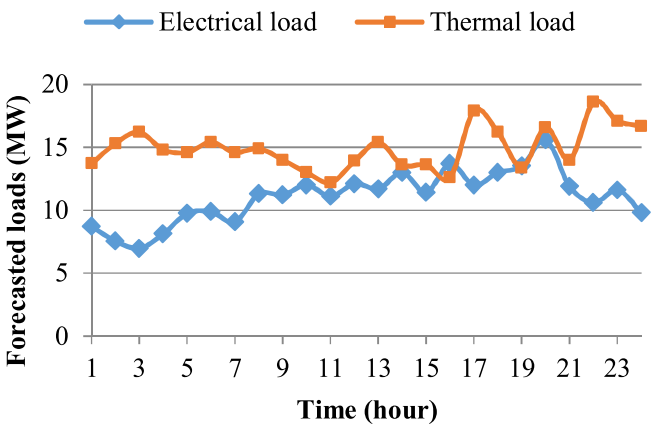

Figure 5: Forecasted energy demand of the microgrid

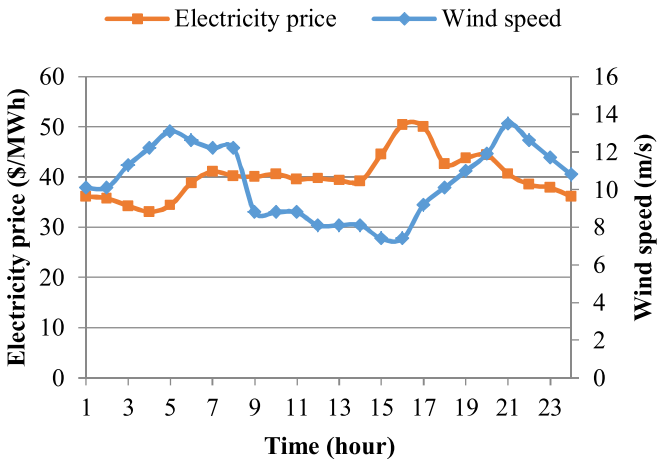

Figure 6: Day-ahead electricity prices and forecasted wind speed

5. Results and Sensitivity Analysis

6.1. Cost analysis

The proposed robust operation method has been applied to the defined 21-node microgrid test system and several analyses have been carried out. The proposed model as described in the solution methodology section has been linearized and optimized using CPLEX solver in GAMS software environment. For simplicity the budgets of uncertainties and the percent of forecast errors are considered as $\Gamma = \Gamma_{PL} = \Gamma_{TL} = \Gamma_{wt}$ and $E = E_{PL} = E_{TL} = E_{wt}$, respectively. The robust operation costs of the microgrid by variation of the budget of uncertainty and the forecast error are illustrated in Figure 7. As expected, by incrementing the budget of uncertainty, in better words the degree of robustness and the forecast error, the operation cost is increased. As shown in this figure, by considering the budget of uncertainty $\Gamma = 0$, the robust model is converted to a deterministic problem with operation cost of \$12488. On the other hand, for values of $\Gamma \geq 24$, since the worst case has occurred, the operation costs are not increased anymore. It means that we can adjust the robustness degree of the solution using the parameter Γ.

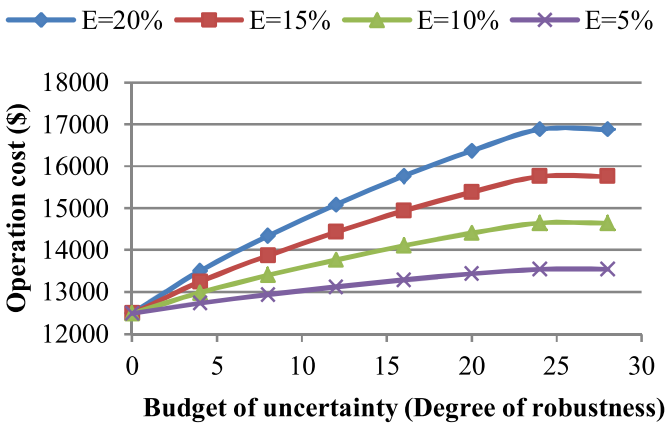

Figure 7: Robust operation costs of the microgrid

6.2. Worst case analysis

Figure 8, Figure 9, and Figure 10 demonstrate the deviation of electrical load, thermal load, and the wind generations for $\Gamma = 12, 24$ from the forecasted values ($\Gamma = 0$), respectively. In this study the forecast errors are considered 20%. It can be seen that the worst case $\Gamma = 24$ occurs in the upper bound of the forecasted electrical and thermal loads while it is in the lower bound of the wind generation. Sine in the condition of the maximum load and the minimum wind generation, the microgrid operation cost dramatically increases. It means that the worst case happens in the state where the auxiliary binary variables in (2)-(4) are $v_{i,PL}^{t+} = v_{i,TL}^{t+} = v_{wt}^{t-} = 1, \forall i \epsilon I, wt \epsilon WT, t \epsilon T$ and the summation over the 24-hours of the day-ahead results in 24. Besides, for the budget of uncertainty $\Gamma = 12$, the degree of robustness is limited and only in the critical hours (i.e. hours 12-21 where the day-ahead electricity price is high) the binary variables take value of 1 that the summation of them in 24 hours will be 12.

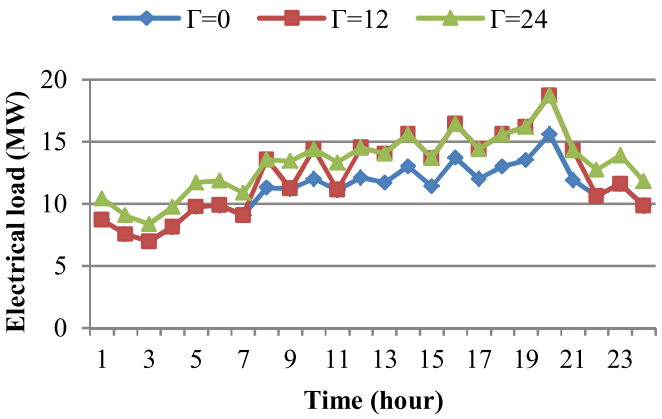

Figure 8: Deviation of electrical load from the forecasted values

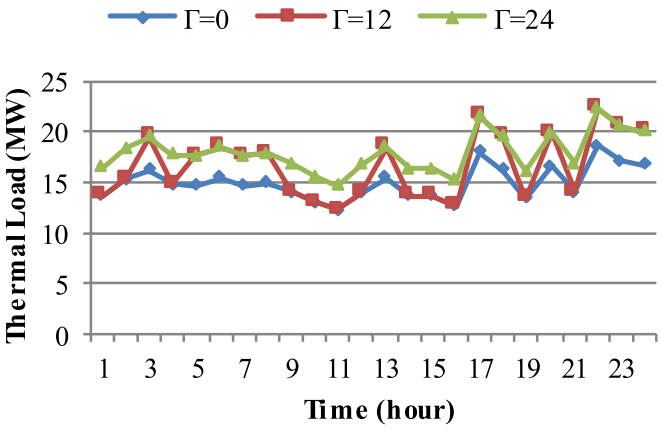

Figure 9: Deviation of thermal load from the forecasted values

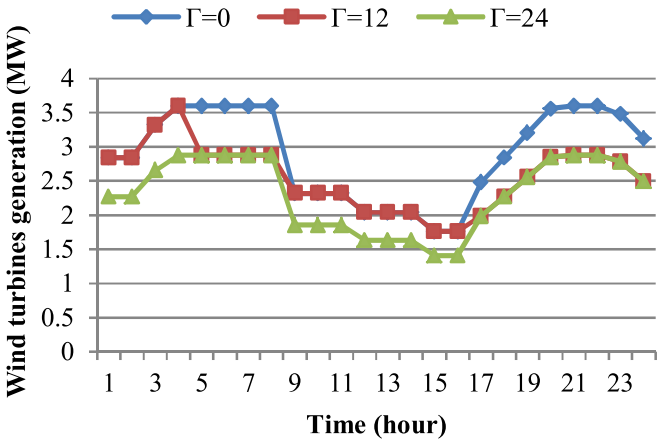

Figure 10: Deviation of wind turbines generation from the forecasted values

6.3. Unit commitment results

The units' commitments are obtained in the first stage of optimization approach. Table 1 compares the day-ahead commitment status of units in node 5 with $\Gamma = 12, 24$ and forecast error of 20% with that of the deterministic model. As shown, the status of CHP is not changed since it has a lower operation cost with respect to procuring energy from the main grid. On the other hand, the boilers are committed in more hours by increasing the model robustness. On the contrary, the heat pumps commitments are based on the electricity price and vary in different hours.

Table 1: Day-ahead commitment status of the units with different budget of uncertainties

	CHP	Boiler	Heat pump
Deterministic	111111111111111111111111	001001011111111111111111	111111111010000010001111
$\Gamma = 12$	111111111111111111111111	001011111111111111111111	111111111010100011010111
$\Gamma = 24$	111111111111111111111111	111111111111111111111111	111111110000100011010111

6.4. Dispatch results

The energy dispatch results are determined in the second stage. The results are based on the dual variables in the sub-problem that cannot be analysed in this manner. In this paper, the worst case condition with $\Gamma = 24$ and forecast error of 20% is implemented in the deterministic model to determine the energy dispatch. As a result, Figure 11 and Figure 12 represent the day-ahead procured electrical and thermal energy, respectively. As shown, the CHPs are procured the whole day due to the low natural gas price. The renewable generation is based on the forecasted values [30] while the other dispatchable resources are scheduled based on their marginal costs. As shown, the price of electricity directly affects the scheduling of electricity and natural gas

network as well as thermal energy supply in the microgrid and once the price of electricity increases, the energy purchased from the main grid is reduced.

Accordingly, Figure 13 demonstrates the state of energy in batteries and heat storages. As expected, batteries are charged in low prices and low demands (i.e., time 3 to 14) and discharged in high prices or peak loads (i.e. time 15 to 20). As shown in this figure, heat storages are stored in low electricity prices (i.e., time 3 to 16) and withdrawn in peak loads and high electricity prices (i.e., time 17 to 21). In other word, heat storages have the same performance as the batteries. Since at peak hours, most natural gas is used to generate electric power by the CHPs. So, due to limitations, there will not be sufficient natural gas to produce thermal energy and heat storages are scheduled to withdraw energy in these hours.

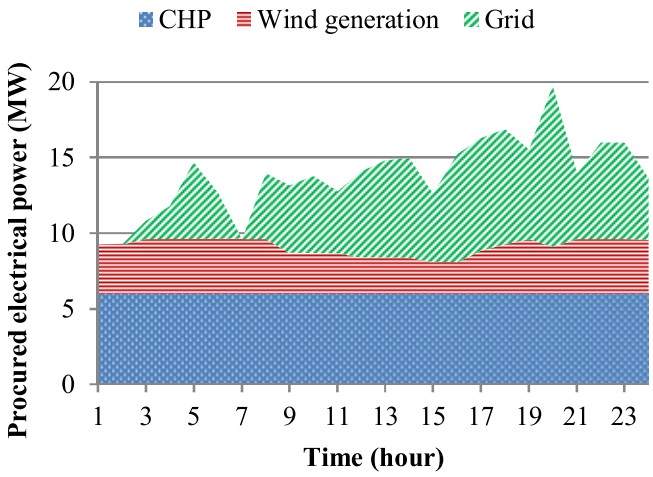

Figure 11: Day-ahead electrical energy scheduling

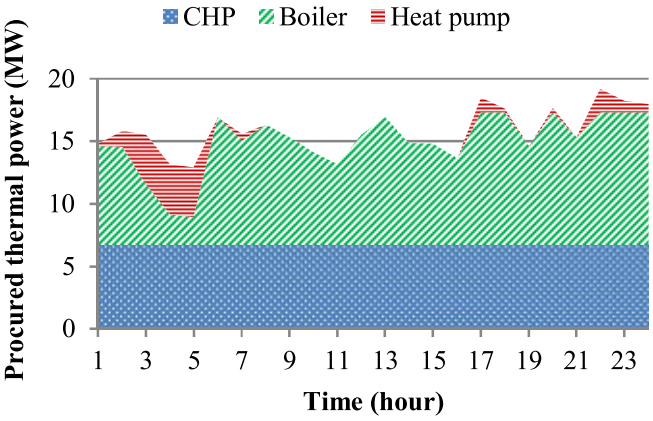

Figure 12: Day-ahead thermal energy scheduling

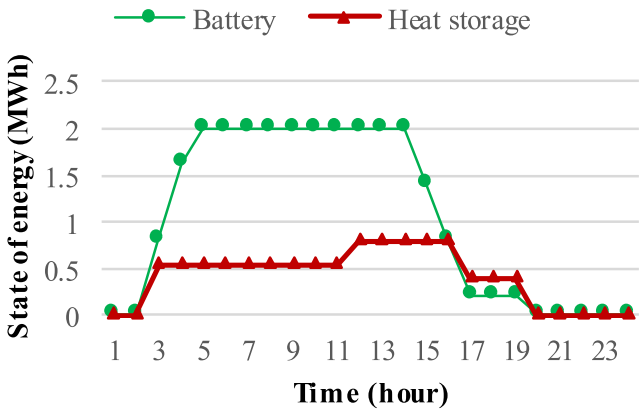

Figure 13: State of energy in batteries and heat storages

Furthermore, the day-ahead variation of the voltage magnitude and pressure of natural gas at node 5 are respectively illustrated in Figure 14 and Figure 15, and compared with that of the deterministic model. As shown, by increasing the model robustness ($\Gamma = 24$), the profile of voltage and natural gas pressure are descended. Moreover, because the natural gas network is radial, the downstream nodes of pipelines (i.e., nodes 9, 14, 17 and 19) have less pressure than the upstream nodes. Besides, during hours 13 to 16, all the nodes have their minimum voltage. Since in these hours, maximum purchasing electricity from the main grid is scheduled because of the low electricity price, and the voltage magnitudes are decreased.

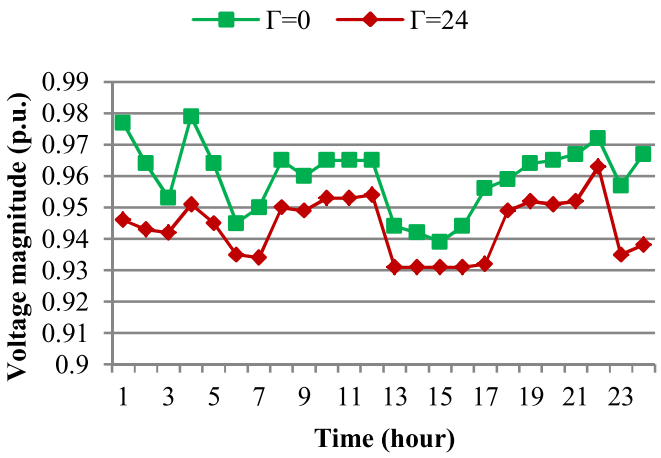

Figure 14: Day-ahead voltage magnitude profile at node 5

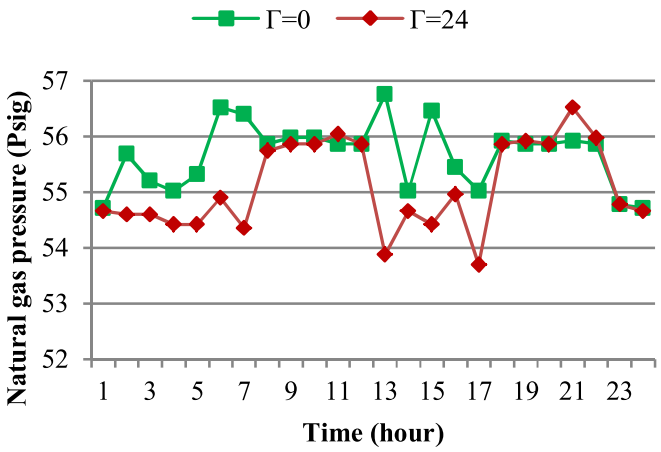

Figure 15: Day-ahead natural gas pressure profile at node 5

6. Conclusion

A robust two-stage operation model of microgrids with natural gas infrastructure and energy hubs was proposed and implemented on a 21-node test microgrid. The proposed *min max min* robust problem was enabled using the C&CG approach that decomposed the framework into a sub-problem and a master problem. The uncertain variables were considered as electrical and thermal loads as well as the wind generation in polyhedral uncertainty sets. The measure of conservativeness of the solution was regulated using the budget of uncertainty parameter that adjusts the degree of robustness using the auxiliary binary variables. It was shown that, by incrementing the budget of uncertainty, at first, the binary variables took the value of 1 in periods with peak loads and peak energy prices. Also, the maximum robustness occurred when the auxiliary binary variables were 1 for all hours with summation equal to 24. It was revealed that by increasing the budget of uncertainty and the forecast error, the operation cost increased up to 35% with respect to the deterministic approach, while the solution would be robust against all realizations of uncertainties. Besides, it was concluded that the degree of robustness affected the scheduling in both electricity and natural gas energy networks. It is observed that the electricity price effects on the procurement of electrical and thermal energy and consequently the loading of both electricity and natural gas networks. It was also shown that the proposed robust method affects the congestion in energy networks. It should be mentioned that the main limitation of the proposed method is associated with the transforming the dual variables to the dispatch variables. Although an approach was utilized to analyse the primal variables including the unit commitment as well as dispatch results, but more approaches can be addressed for future works.

Appendix

The specification of resources in the microgrid and energy hubs is illustrated in Table 2. The distribution lines data and pipelines specifications are summarized in Table 3. Furthermore, the thermal and electrical loads ratios are demonstrated in Table 4. It should be mentioned that in this paper the electrical load power factors are set to 0.85.

Table 2: Characteristics of resources

Units	Connecting Node	Characteristics			
CHP	5,9,14	$\eta_{CHP,e/h}$ [%] 42/47	$P_{n,e/h}^{min}$ [MW] 0.4	$P_{n,e/h}^{max}$ [MW] 4	KU_n [$] 10
Heat Storage	5	ES_{hs}^{min} [MWh] 0.1	ES_{hs}^{max} [MWh] 1	$P_{hs}^{st,max}$ [MW] 0.4	$P_{hs}^{wd,max}$ [MW] 0.6
Boiler	2,5,9,14,17,19	η_{bo} [%] 85	P_{bo}^{min} [MW] 0	P_{bo}^{max} [MW] 1.5	KU_{bo} [$] 10
Heat Pump	4,5,6,7,11,13,15,21	COP_{hp} 1.5	P_{hp}^{min} [MW] 0	P_{hp}^{max} [MW] 0.5	KU_{hp} [$] 0.5
Wind Turbines	10,12,20	$P_{wt,r}$ [MW] 1.2	v_{cin} [m/s] 3	v_{cout} [m/s] 50	v_r [m/s] 12
Battery	3,8	SOC_b^{min} [MWh] 0.1	SOC_b^{max} [MWh] 1	$P_b^{ch,max}$ [MW/h] 0.6	$P_b^{dis,max}$ [MW/h] 0.6

Table 3: Distribution lines data and pipelines specification

Node from-to	Resistance (p.u)	Reactance (p.u)	Susceptance (p.u)	Max. Current (A)	k_{ij} pipelines
1-2	0.0092	0.0050	0.0038	340	
2-3	0.0133	0.0058	0.0039	290	
2-5	-	-	-	-	9
2-10	0.0392	0.0171	0	190	
3-4	0.0143	0.0158	0	380	
4-5	0.0131	0.0137	0	295	
4-11	0.0110	0.0078	0	260	
5-6	0.0123	0.0127	0	295	
5-9	-	-	-	-	8.25
5-14	-	-	-	-	7
5-17	-	-	-	-	7.2
6-7	0.0214	0.0151	0	260	
7-8	0.0207	0.0146	0	260	
7-16	0.0124	0.0088	0	260	
8-9	0.0249	0.0109	0	190	
9-19	-	-	-	-	6
8-20	0.0238	0.0104	0	190	
11-12	0.0234	0.0166	0	260	
11-13	0.0238	0.0104	0	190	
13-14	0.0380	0.0166	0	190	
14-15	0.0333	0.0145	0	190	
16-17	0.0114	0.0037	0.0022	245	
16-18	0.0273	0.0119	0	190	
18-19	0.0368	0.0160	0	190	
20-21	0.0356	0.0155	0	190	

Table 4: Load ratios of nodes

Node Number	Electric Load	Thermal Load	Node Number	Electric Load	Thermal Load
2	0.057	0.072	**12**	0.036	0
3	0.066	0	**13**	0.049	0.021
4	0.066	0.015	**14**	0.043	0.206
5	0.064	0.162	**15**	0.033	0.034
6	0.052	0.032	**16**	0.039	0
7	0.039	0.026	**17**	0.044	0.108
8	0.056	0	**18**	0.043	0
9	0.044	0.202	**19**	0.033	0.071
10	0.069	0	**20**	0.066	0
11	0.055	0.017	**21**	0.044	0.034

References

[1] M. Geidl and G. Andersson, "Optimal Power Flow of Multiple Energy Carriers," *IEEE Transactions on Power Systems,* vol. 22, no. 1, pp. 145-155, 2007, doi: 10.1109/TPWRS.2006.888988.

[2] Z. Li and Y. Xu, "Optimal coordinated energy dispatch of a multi-energy microgrid in grid-connected and islanded modes," *Applied Energy,* vol. 210, pp. 974-986, 2018.

[3] T. Ma, J. Wu, and L. Hao, "Energy flow modeling and optimal operation analysis of the micro energy grid based on energy hub," *Energy conversion and management,* vol. 133, pp. 292-306, 2017.

[4] A. Najafi, H. Falaghi, J. Contreras, and M. Ramezani, "Medium-term energy hub management subject to electricity price and wind uncertainty," *Applied Energy,* vol. 168, pp. 418-433, 2016.

[5] B. Zhao, A. J. Conejo, and R. Sioshansi, "Unit commitment under gas-supply uncertainty and gas-price variability," *IEEE Transactions on Power Systems,* vol. 32, no. 3, pp. 2394-2405, 2017.

[6] M. S. Javadi, M. Lotfi, A. E. Nezhad, A. Anvari-Moghaddam, J. M. Guerrero, and J. P. Catalão, "Optimal Operation of Energy Hubs Considering Uncertainties and Different Time Resolutions," *IEEE Transactions on Industry Applications,* 2020.

[7] S. A. Mansouri, A. Ahmarinejad, M. S. Javadi, and J. P. Catalão, "Two-stage stochastic framework for energy hubs planning considering demand response programs," *Energy,* vol. 206, p. 118124, 2020.

[8] M. Kia, M. Shafiekhani, H. Arasteh, S. Hashemi, M. Shafie-khah, and J. Catalão, "Short-term operation of microgrids with thermal and electrical loads under different uncertainties using information gap decision theory," *Energy,* vol. 208, p. 118418, 2020.

[9] M. H. Shams, M. Shahabi, and M. E. Khodayar, "Stochastic day-ahead scheduling of multiple energy carrier microgrids with demand response," *Energy,* vol. 155, pp. 326-338, 2018.

[10] M. H. Shams, M. Shahabi, and M. E. Khodayar, "Risk-averse optimal operation of Multiple-Energy Carrier systems considering network constraints," *Electric Power Systems Research,* vol. 164, pp. 1-10, 2018.

[11] D. Bertsimas and M. Sim, "The price of robustness," *Operations research,* vol. 52, no. 1, pp. 35-53, 2004.

[12] N. Amjady, S. Dehghan, A. Attarha, and A. J. Conejo, "Adaptive robust network-constrained AC unit commitment," *IEEE transactions on power systems,* vol. 32, no. 1, pp. 672-683, 2016.

[13] A. Attarha, N. Amjady, and A. J. Conejo, "Adaptive robust AC optimal power flow considering load and wind power uncertainties," *International Journal of Electrical Power & Energy Systems,* vol. 96, pp. 132-142, 2018.

[14] R. Jiang, J. Wang, and Y. Guan, "Robust unit commitment with wind power and pumped storage hydro," *IEEE Transactions on Power Systems,* vol. 27, no. 2, pp. 800-810, 2011.

[15] A. Lorca and X. A. Sun, "Adaptive robust optimization with dynamic uncertainty sets for multi-period economic dispatch under significant wind," *IEEE Transactions on Power Systems,* vol. 30, no. 4, pp. 1702-1713, 2014.

[16] T. Soares, R. J. Bessa, P. Pinson, and H. Morais, "Active distribution grid management based on robust AC optimal power flow," *IEEE Transactions on Smart Grid,* vol. 9, no. 6, pp. 6229-6241, 2017.

[17] A. Gholami, T. Shekari, and S. Grijalva, "Proactive management of microgrids for resiliency enhancement: An adaptive robust approach," *IEEE Transactions on Sustainable Energy,* 2017.

[18] Y. Zhang, N. Gatsis, and G. B. Giannakis, "Robust energy management for microgrids with high-penetration renewables," *IEEE Transactions on Sustainable Energy,* vol. 4, no. 4, pp. 944-953, 2013.

[19] G. Liu, M. Starke, B. Xiao, and K. Tomsovic, "Robust optimisation-based microgrid scheduling with islanding constraints," *IET Generation, Transmission & Distribution,* vol. 11, no. 7, pp. 1820-1828, 2017.

[20] C. Zhang, Y. Xu, Z. Li, and Z. Y. Dong, "Robustly coordinated operation of a multi-energy microgrid with flexible electric and thermal loads," *IEEE Transactions on Smart Grid,* 2018.

[21] M. Shahidehpour, M. Yan, X. Ai, J. Wen, N. Zhang, and C. Kang, "Robust two-stage regional-district scheduling of multi-carrier energy systems with a large penetration of wind power," *IEEE Transactions on Sustainable Energy,* 2018.

[22] C. He, L. Wu, T. Liu, and M. Shahidehpour, "Robust co-optimization scheduling of electricity and natural gas systems via ADMM," *IEEE Transactions on Sustainable Energy,* vol. 8, no. 2, pp. 658-670, 2017.

[23] Y. He, M. Shahidehpour, Z. Li, C. Guo, and B. Zhu, "Robust Constrained Operation of Integrated Electricity-Natural Gas System Considering Distributed Natural Gas Storage," *IEEE Transactions on Sustainable Energy,* 2017.

[24] D. Bertsimas, E. Litvinov, X. A. Sun, J. Zhao, and T. Zheng, "Adaptive robust optimization for the security constrained unit commitment problem," *IEEE transactions on power systems,* vol. 28, no. 1, pp. 52-63, 2012.

[25] N. Amjady, S. Dehghan, A. Attarha, and A. J. Conejo, "Adaptive robust network-constrained AC unit commitment," *IEEE Transactions on Power Systems,* vol. 32, no. 1, pp. 672-683, 2017.

[26] M. E. Khodayar, M. Barati, and M. Shahidehpour, "Integration of high reliability distribution system in microgrid operation," *IEEE Transactions on Smart Grid,* vol. 3, no. 4, pp. 1997-2006, 2012.

[27] B. Zeng and L. Zhao, "Solving two-stage robust optimization problems using a column-and-constraint generation method," *Operations Research Letters,* vol. 41, no. 5, pp. 457-461, 2013.

[28] M. Shahidehpour and Y. Fu, "Benders decomposition in restructured power systems," *IEEE Techtorial,* no. April, 2005.

[29] M. Mansour-lakouraj and M. Shahabi, "Comprehensive analysis of risk-based energy management for dependent micro-grid under normal and emergency operations," *Energy,* vol. 171, pp. 928-943, 2019.

[30] M. H. Shams, M. Kia, A. Heidari, and D. Zhang, "Optimal design of photovoltaic solar systems considering shading effect and hourly radiation using a modified PSO algorithm," *SIMULATION,* vol. 95, no. 10, pp. 931-939, 2019, doi: 10.1177/0037549719831362.